RSC Advances

PAPER

View Article Online
View Journal | View Issue

Cite this: *RSC Adv.*, 2017, **7**, 40563

Perimidine based selective colorimetric and fluorescent turn-off chemosensor of aqueous Cu^{2+}: studies on its antioxidant property along with its interaction with calf thymus-DNA†

Debashis Roy,[a] Arijit Chakraborty *[b] and Rina Ghosh *[a]

Received 15th June 2017
Accepted 10th August 2017

DOI: 10.1039/c7ra06687b

rsc.li/rsc-advances

We have developed a perimidine based simple and easily synthesised chemosensor, 1,3-bis(2,3-dihydro-1*H*-perimidin-2-yl)benzene (**1**), which exhibits selective colorimetric and fluorescence "turn off" response toward nano molar Cu^{2+}. This method allows a sensitive readout of chemosensor **1** within a wide linear range of (5–2771) $\times$ 10^{-8} M at λ_{max} 346 nm, and with limit of detection (LOD) 6.19 $\times$ 10^{-8} M. Moreover, **1** exhibits free radical scavenging ability, six times better than that of L-ascorbic acid. The binding interaction studies of **1** with calf-thymus DNA (CT-DNA) indicate a groove binding mode.

1. Introduction

Cu^{2+} ions play a vital role in many biological processes such as haemopoiesis, various enzyme catalyzed biochemical reactions *e.g.* transformation of melanin for pigmentation of the skin and assistance of the formation of crosslinks in collagen and elastin[1,2] and assistance in iron absorption. Unregulated overloading of Cu^{2+} can lead to lethargy, vomiting, increased blood pressure and respiratory rates, liver damage, acute haemolytic anaemia, neurotoxicity, and neurodegenerative diseases including Alzheimer's, Parkinson's and prion diseases.[3–5] Furthermore, Cu^{2+} can entangle natural ecosystems owing to its adverse effects on micro-organisms.[6] According to U. S. Environmental Protection Agency (EPA) the consumption limit of Cu^{2+} in drinking water should not exceed 1.3 ppm ($\sim$20 μM).[7,8] For the last 10–20 decades, Cu^{2+} pollution has underscored major problems all over the world due to the enormous use of Cu^{2+} based complexes in agriculture and industry.[9] Therefore, the development of selective, sensitive, efficient and believable detection methods of aqueous Cu^{2+} ions have drawn a significant interest to the scientific and environmental communities.

Previously, the quantification of the Cu^{2+} was done *via* a number of analytical methods including atomic absorption/emission spectroscopy (AAS/AES),[10] electrochemical methods,[11] inductively-coupled plasma mass spectrometry (ICPMS) and X-ray fluorescence spectroscopy (XRF).[12] Nevertheless, these techniques of quantification of the Cu^{2+} involve the use of sophisticated instrumentation, time consuming sample pre-treatment and separation methods, thus making these inconvenient for the fast detection of aqueous Cu^{2+} ions.

In current period, all these techniques have been mitigated by new colorimetric as well as spectro-photometric methods. The techniques depend upon UV-vis absorption and fluorescence measurements of fluorophore moieties[13–15] which can act as high performance chemo-sensors for metal ion detection. These have drawn much attention for several advantages such as high sensitivity, selectivity and comfortable operation in identifying the metal ions.

Free-radicals play an important role in the oxidative damage of organisms.[16,17] An antioxidant is a chemical species that prevents the oxidation of the free-radicals. The oxidative stress induced by reactive oxygen species (ROS) is portrayed as a dynamic imbalance between the levels of free radicals generated in the body and quantity of antioxidants to scavenge them and protect against their harmful effects.[18] Increasing amounts of ROS become harmful because these can initiate bio-molecular oxidation which causes cell injury and cell death; oxidative stress leads to countless diseases and disorders such as cataracts, aging, cirrhosis, cancer and atherosclerosis.[19] Therefore, an evaluation of antioxidant properties of pure organic compounds is also very important because of their uses in various commodities[20] and chemical reactions. DPPH assay is well-known assessment of free radical scavenging by an antioxidant and believed as one of the standard and easy colorimetric methods for the estimation of antioxidant properties of pure organic compounds.[21] Herein, we are reporting our recent studies on the selective colorimetric and fluorimetric sensing of a perimidine based compound for detection of nanomolar aqueous Cu^{2+} solution; the free radical scavenging and the binding of the chemo-sensor with CT-DNA will also be demonstrated.

[a]*Department of Chemistry, Jadavpur University, Kolkata 700032, India. E-mail: roy.debashis89@gmail.com; ghoshrina@yahoo.com*

[b]*Department of Chemistry, Acharya B. N. Seal College, Cooch Behar, West Bengal 736101, India. E-mail: arijit_chak2002@yahoo.com*

† Electronic supplementary information (ESI) available. See DOI: 10.1039/c7ra06687b

2. Experimental

2.1. General information

All the solvents and reagents used were of analytical grade and spectroscopic grade. The salts used as metal ions source were $AgNO_3$, $Ba(NO_3)_2$, $Ca(NO_3)_2 \cdot 4H_2O$, $Cd(NO_3)_2$, $Co(NO_3)_2 \cdot 6H_2O$, $Cr(NO_3)_3$, $Cu(NO_3)_2 \cdot 3H_2O$, $(NH_4)_2Fe(SO_4)_2 \cdot 6H_2O$, $HgNO_3$, $MnSO_4 \cdot H_2O$, $NaNO_3$, $Ni(NO_3)_2 \cdot 6H_2O$, $Pb(NO_3)_2$ and $ZnSO_4 \cdot 7H_2O$. ^1H NMR and ^{13}C NMR measurements were performed on a Bruker DPX-300 (300 and 75 MHz, respectively) spectrometer, and chemical shifts were recorded in ppm. FT-IR data were taken from PerkinElmer Spectrum Version 10.03.09. A high-resolution mass spectrum was obtained on a Waters Micromass Q-tof Micro mass spectrometer using electrospray ionization method. Melting points were determined on a LabX India digital melting point apparatus. UV-vis spectra were recorded at room temperature using a PerkinElmer UV Lambda 25 spectrometer, and fluorescence data were collected from PerkinElmer fluorescence Spectrometer LS 55. Time resolved fluorescence decay measurements were recorded in Horiba-Jobin Yvon FluoroCube fluorescence lifetime system using NanoLED at 330 nm (IBH, UK) as the excitation source and TBX photon detection module as the detector. Circular dichroism (CD) spectral measurements were run on a PC-driven JASCO J815 spectropolarimeter (Jasco International Co., Hachioji, Japan) with an attached temperature controller using a rectangular quartz cuvette of 1 cm path length.

2.2. Synthesis of 1,3-bis(2,3-dihydro-1*H*-perimidin-2-yl) benzene (1)[22]

Isophthalaldehyde (1 g, 7.46 mmol) and 1,8-diaminonaphthalene (2.3587 g, 14.9 mmol) were added to 30 mL of ethanol, and the reaction mixture was refluxed for 4 hours. A rosy brown solid product was separated out from the reaction medium, and the product was filtered and washed with ethanol, distilled water and dichloro methane, successively for 2 times to get pure product. Yield: 2.9374 g (95%). Mp = 224 °C.

IR spectrum (cm^{-1}, KBr pellet): 3370 (NH str.), 3044 (CH str.), 1597 (C=C str.), 1482, 1425, 1414, 1252, 815, 760.^1H NMR ($CDCl_3$, 300 MHz): δ 7.96 (1H, s, H-Ar), 7.72 (2H, d, $J = 7.4$, H-Ar), 7.52 (1H, t, $J = 7.6$, H-Ar), 6.54–6.56 (4H, m, H-Ar), 5.54 (2H, s, CH), 4.54 (2H, br, s, NH), 1.63 (2H, br, s, NH). ^{13}C NMR (75 MHz, $CDCl_3$): δ 141.9, 141.0, 134.9, 129.4, 129.0, 127.3, 126.9, 118.1, 113.5, 106.0, 68.1. HRMS: found $[M + H]^+$ 415.1914; 'molecular formula $C_{28}H_{22}N_4$' requires $[M + H]^+$415.1923.

2.3. UV-vis titration of 1 with Cu^{2+} ion[23,24]

6.26 mM solution of **1** in acetonitrile and 2.5 mM solution of $Cu(NO_3)_2 \cdot 3H_2O$ in water were prepared as stock solutions. 2 μL of **1** (6.26 mM) was diluted to 2 mL acetonitrile in a cuvette, and the UV-vis spectrum was run. Then 2 μL of Cu^{2+} solution (2.5 mM) was added to the same cuvette; after mixing these homogeneously, UV-vis absorption spectrum was run at room temperature. This process of addition of Cu^{2+} solution (2.5 mM) was repeated for several times upto saturation.

2.4. Fluorescence spectroscopic titration of 1 with Cu^{2+} ion[25,26]

5 μL of the **1** (0.25 mM) was diluted to 2 mL acetonitrile, and 1 μL of the aqueous Cu^{2+} solution (0.25 mM) was added each time to the diluted **1** solution. After mixing homogeneously, fluorescence spectra were recorded at room temperature by exciting **1** at 346 nm. This process was run for several times upto saturation.

2.5. Job plot measurements of 1 with Cu^{2+} ion[23]

A solution (5 mM) of **1** in acetonitrile and a Cu^{2+} (copper nitrate trihydrate) solution (5 mM) in water were prepared as stock solutions. Then 1, 2, 3, 4, 5, 6, 7, 8 and 9 μL from the stock solution of **1** were taken and transferred to different vials. 9, 8, 7, 6, 5, 4, 3, 2 and 1 μL of the Cu^{2+} solution (5 mM) were added respectively, to the above mentioned vials so that the mole fraction of **1** in each vial became 0.1, 0.2, 0.3, 0.4, 0.5, 0.6, 0.7, 0.8 and 0.9, respectively. Each vial was diluted with acetonitrile to make a total volume of 2 mL. After shaking the vials for a few seconds to form **1**-Cu^{2+} complex, UV-vis absorption spectra were recorded at 25 °C. Similar process was run for blank test with solution of **1** only.

2.6. pH dependency of 1[27]

A series of buffer solutions with pH values ranging from 1 to 10 were prepared. 2 μL of a solution (2 mM) of **1**, prepared in acetonitrile, was added to 2 mL buffer of each pH. After mixing it homogeneously, fluorescence spectra (excited at 346 nm) were recorded for all pH ranging from 1 to 10 at room temperature.

2.7. Evaluation of antioxidant activity by DPPH assay[21]

Step 1: 0.01 (M) methanolic solution of each of **1**, DPPH (1,1-diphenyl-2-picrylhydrazyl) and L-ascorbic acid were prepared by accurate weighing. Then, the solution of **1** was serially diluted to 1/2, 1/4, 1/8, 1/16 and 1/32.

Step 2: to seven sample vials 10 μL of 0.01 (M) DPPH solution was added. Among these, to the six sample vials 10 μL of serially diluted solutions of **1** prepared in step 1, was added. To the rest sample vial 10 μL of methanol was added. This seventh vial served as the blank. Then the content of each vial was diluted to 2 mL. After mixing homogenously, these seven solutions were allowed to react for 40 minutes at room temperature under dark. UV-vis absorption spectra of the seven solutions were run at room temperature, and the corresponding absorbance values were read at 517 nm.

Step 3: similar procedure of step 2 was also followed for L-ascorbic acid as standard.

2.8. UV-vis titration of 1 with CT-DNA[28]

5 mM solution of **1** in acetonitrile and 1 mM solution of CT-DNA in citrate-phosphate buffer of pH 7 were prepared as stock solutions. 5 μL of the stock solution of **1** was diluted to 2 mL citrate-phosphate buffer (pH 7) in cuvette, and the UV-vis spectrum was taken. Then 5 μL of CT-DNA (1 mM) solution was added to the same cuvette, after mixing these

homogeneously, UV-vis absorption spectrum was run at room temperature. This process of addition of CT-DNA solution (1 mM) was repeated for several times upto saturation.

2.9. Fluorescence spectroscopic titration of 1 with CT-DNA[29]

2 μL of the **1** (5 mM) was diluted to 2 mL citrate-phosphate buffer of pH 7, and 2 μL of the CT-DNA (1 mM) solution was added each time to the diluted solution of **1**. After mixing homogeneously, fluorescence spectra were recorded at room temperature by exciting **1** at 346 nm. This process was run for several times upto saturation.

3. Results and discussion

3.1. Synthesis and characterisation

The chemo-sensor **1** was synthesised by coupling of iso-phthalaldehyde with 1,8-diaminonaphthalene in absolute ethanol at refluxing condition following literature procedure[22] with some modification (Scheme 1); a better yield of **1** was obtained by this modification. Compound **1** was characterised by ^{1}H NMR, ^{13}C NMR, FT-IR and high resolution mass spectrometry (Fig. S1–S4, ESI†).

3.2. Visual and spectral changes of chemosensor 1 towards cations

Due to the poor solubility of compound **1** in water, the colorimetric sensing abilities of **1** were investigated in acetonitrile medium (40 μM) upon the treatment with various kinds of aqueous cations such as Ag^{+}, Ba^{2+}, Ca^{2+}, Cd^{2+}, Co^{2+}, Cr^{3+}, Cu^{2+}, Fe^{2+}, Hg^{+}, Mn^{2+}, Na^{+}, Ni^{2+}, Pb^{2+} and Zn^{2+}. To examine the spectral changes of **1** toward cations, a solution of **1** was treated with above mentioned cations (Fig. 1).

Upon the addition of aqueous Cu^{2+} to the solution of **1** (6.25 μM, λ_{max} = 346 nm, molar extinction co-efficient (ε) = 2.72×10^{4} M^{-1} cm^{-1} in acetonitrile), a change of colourless to chocolate colour was observed; other cations did not produce any visual change. Subsequently a change in the UV-vis absorption peak with a bathochromic shift at 475 nm and isosbestic points at 239 nm, 301 nm and 357 nm indicate the formation of a stable complex with Cu^{2+} ion (Fig. 1). Thus compound **1** is no-doubt a potential candidate for "naked-eye" chemo-sensor of Cu^{2+} ion.

To establish fluorescent properties of **1** toward aqueous Cu^{2+}, the emission changes were investigated. Upon gradual addition of aqueous Cu^{2+} to the solution of **1** in acetonitrile medium, an amazing fluorescent quenching was observed with quenching efficiency = 93% (Fig. 2).[30]

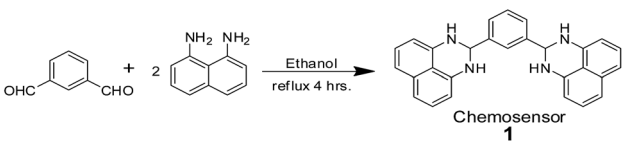

Scheme 1 Synthesis of chemo-sensor **1**.

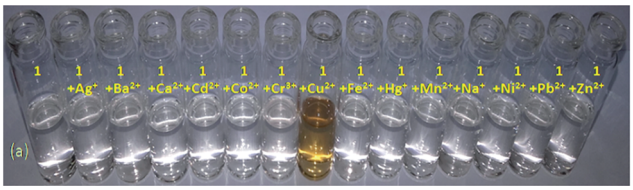

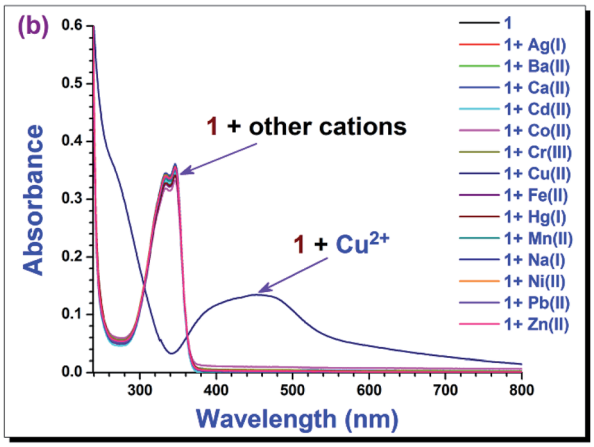

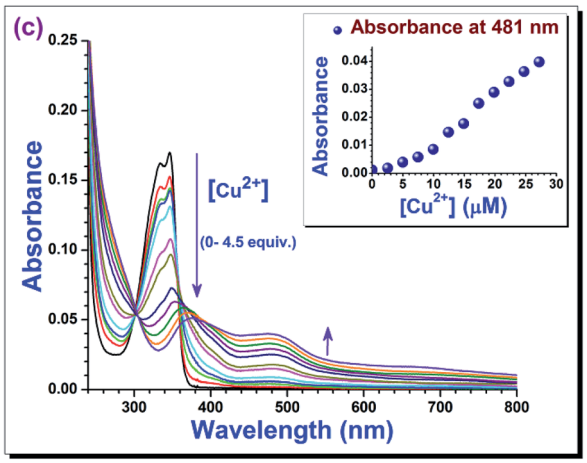

Fig. 1 (a) The color changes of **1** (40 μM) upon addition of various aqueous cations (1 equiv.) in MeCN medium. (b) Absorption changes of **1** (12.86 μM) upon the addition of various aqueous cations (5 equiv.) in MeCN medium at room temperature. (c) Absorption changes of **1** (6.25 μM) upon the addition of aqueous Cu^{2+} (4.5 equiv.) in MeCN medium at room temperature. Inset: absorbance changes of **1** at 481 nm as a function of various aqueous Cu^{2+} ion concentrations.

For collisional quenching the dramatic decrease in intensity was described by the well-known Stern–Volmer equation (eqn (1)):[31]

$$\frac{I_0}{I} = 1 + K_{S-V}[Cu^{2+}] \quad (1)$$

in this equation I_0 and I are the fluorescence intensities, respectively, in the absence of and at the intermediate of the interaction of analyte ions; $[Cu^{2+}]$ is the concentration of analyte ion; K_{S-V} is the Stern–Volmer quenching constant with value 1.5×10^{6} M^{-1} for Cu^{2+}.

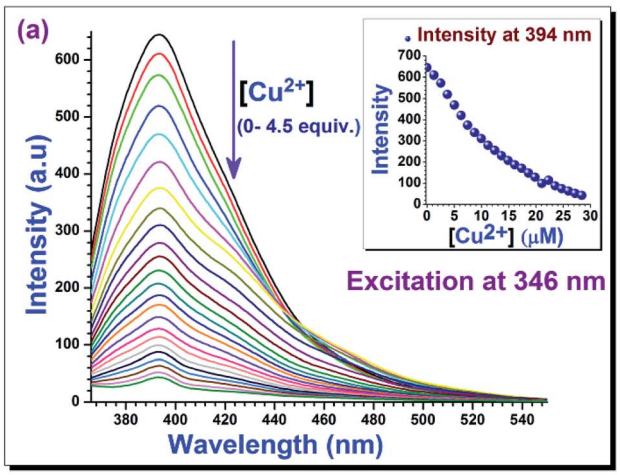

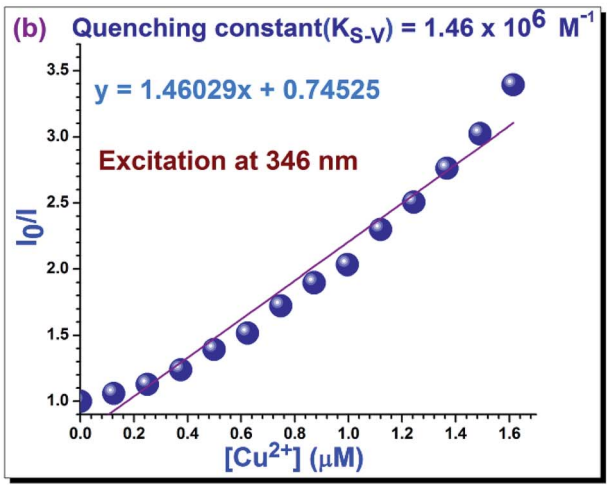

Fig. 2 (a) Fluorescent spectra of **1** (0.62 μM) upon addition of aqueous Cu^{2+} (upto 4.5 equiv.) in MeCN medium. Inset: intensity changes of **1** at 394 nm as a function of various aqueous Cu^{2+} ion concentrations. (b) Stern–Volmer plot for calculation of quenching constant of **1** for Cu^{2+} ion.

3.3. Determination of binding constant

The extent of the binding of **1** toward aqueous Cu^{2+} ion is calculated from an experimental plot of the absorption data using the Benesi–Hildebrand relation (eqn (2)).[32] According to this relation

$$\frac{1}{A - A_0} = \frac{1}{A_f - A_0} + \frac{1}{K_a[Cu^{2+}]\ (A_f - A_0)}$$

$$\frac{(A_f - A_0)}{(A - A_0)} = 1 + \frac{1}{K_b[Cu^{2+}]}$$

$$\log\left(\frac{A_f - A_0}{A - A_0}\right) = -(\log K_b + \log[Cu^{2+}])$$

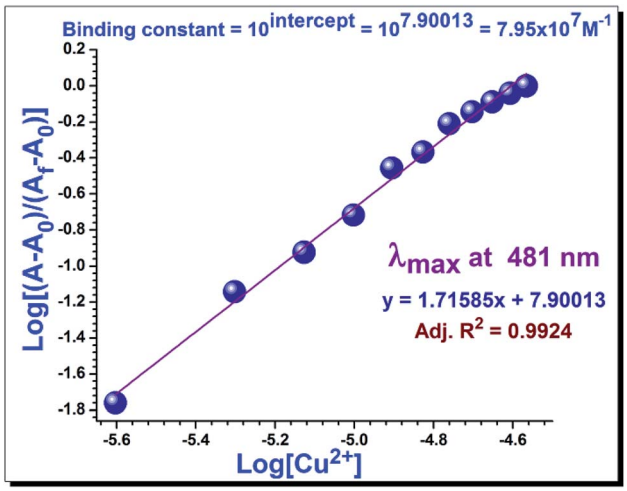

Fig. 3 Benesi–Hildebrand plots for determination of binding constant of **1** for Cu^{2+} ion.

$$\log\left(\frac{A - A_0}{A_f - A_0}\right) = \log[Cu^{2+}] + \log K_b \quad (2)$$

in which A_0, A and A_f are the absorption values, in the absence of, at the intermediate and at the saturation of the interaction of Cu^{2+} ion respectively, and $[Cu^{2+}]$ represents the concentration of aqueous Cu^{2+} ion added. The binding constant (K_b) was determined by linear fitting of absorption titration curve (Fig. 3). The higher value of binding constant ($7.95 \times 10^7\ M^{-1}$) indicates the strong interaction between **1** and Cu^{2+} ion.

3.4. Job plot analysis

The Job plot analysis (Fig. 4a) disclosed a 1 : 1 stoichiometric ratio between **1** and Cu^{2+} ion when difference in absorption maxima were plotted against mole fraction of **1**.[33] This was further corroborated by the mass spectrum (Fig. 4b) of a mixture of **1** and Cu^{2+} in acetonitrile (1 : 1).

3.5. Determination of detection limits[34]

Using UV-vis titration experiment of **1** in acetonitrile solution with aqueous Cu^{2+} (Fig. S6, ESI†), the detection limit was calculated using the equation: detection limit = $3\sigma/m$, where σ is the standard deviation of the blank solution (6.25 μM solution of **1** in acetonitrile only, O.D. at 346 nm), and m is the slope of the intensity *versus* $[Cu^{2+}]$ calibration curve. The detection limits of **1** toward Cu^{2+} ion is 6.19×10^{-8} M.

3.6. Life time measurement

We measured the consequence of aqueous Cu^{2+} on the fluorescence decay behaviour of **1** (Fig. 5). The mean fluorescence lifetime of **1** in acetonitrile was 0.912 ns whereas, a shorter mean fluorescence lifetime 0.639 ns was observed in the presence of Cu^{2+} ion. We have also calculated the radiative rate constant (k_r) and the total non-radiative rate constant (k_{nr}) of **1** and (1 + Cu^{2+}) using the following equations:[35]

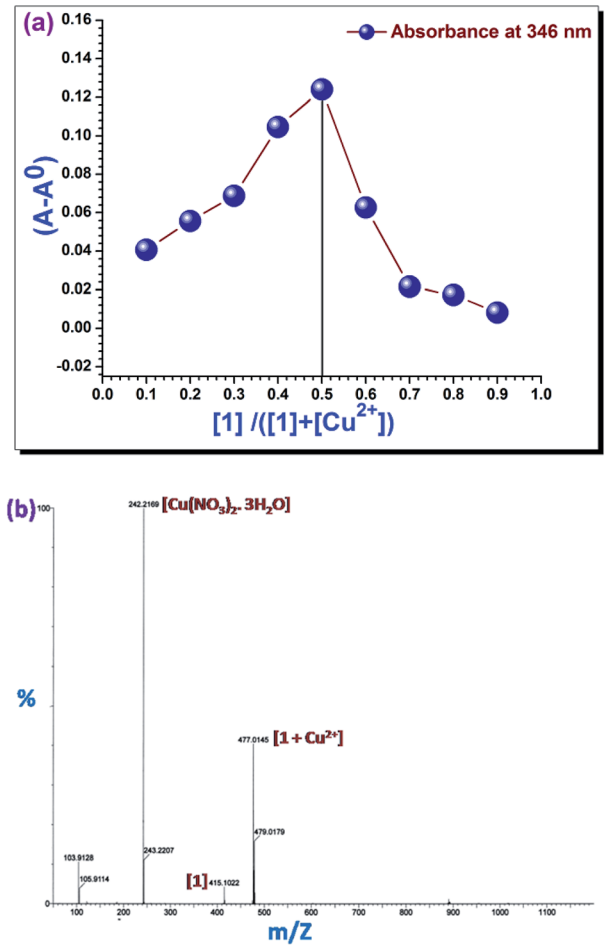

Fig. 4 (a) Job plots for the binding of **1** with Cu^{2+}: $(A - A_0)$ at 346 nm was plotted as a function of the molar ratio [**1**]/([**1**] + [Cu^{2+}]). (b) Positive-ion electrospray ionization mass spectrum of **1** upon addition of 1 equiv. of Cu^{2+} in MeCN.

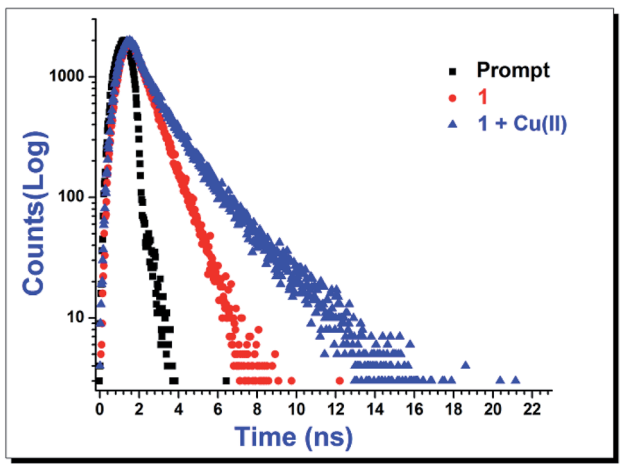

Fig. 5 Time-resolved fluorescence decay curves (logarithm of normalized intensity *vs.* time in ns) of **1** in the absence and presence of aqueous Cu^{2+} ion (3 equiv.).

$$\tau^{-1} = k_r + k_{nr} \quad (3)$$

$$k_r = \Phi/\tau \quad (4)$$

where τ, k_r, k_{nr} and Φ are the mean fluorescence lifetime, radiative rate constant, non-radiative rate constant and fluorescence quantum yield, respectively. All photo-physical parameters are calculated using eqn (3) and (4) (tabulated in Table S1, ESI†). These data indicate that there is small change (1.6 times) in k_{nr} values of **1** and (**1** + Cu^{2+}) whereas almost 12 times decrease has been observed in k_r value for (**1** + Cu^{2+}). Strong chelation between Cu^{2+} and **1** is responsible for such high values which can also be manifested from the high binding constant value.

3.7. Quantum yield measurements[36,37]

Quantum yield of **1** was measured by a secondary method using fluorescence spectra of **1** in the absence and in the presence of aqueous Cu^{2+} in acetonitrile medium using eqn (5), where OD_s and OD_{ref} are the absorbances, and A_s and A_{ref} are integrated emission areas of **1** and standard, respectively. A quantum yield 0.54, for quinine sulfate dihydrate in 0.1 N H_2SO_4, has been used as a standard. The quantum yield of **1** and **1** + Cu^{2+} are 0.1 and 0.0058, respectively.

$$\Phi_s = \frac{OD_{ref} A_s \eta_s^2}{OD_s A_{ref} \eta_{ref}^2} \Phi_{ref} \quad (5)$$

On absorbing photon the fluorophore **1** initiates radiating from the new excited singlet electronic state. During this time, the fluorophore **1** undergoes conformational changes and is also subject to interactions with its molecular environment. The energy of the excited state is partially dissipated, yielding a relaxed singlet excited state from which fluorescence emission originates. In case of **1**, most of the absorbed energy may be engaged in conformational changes and also for the interaction with environment. Hence, lower amount of energy is emitted giving lower value of quantum yield for **1** only. The decrease in

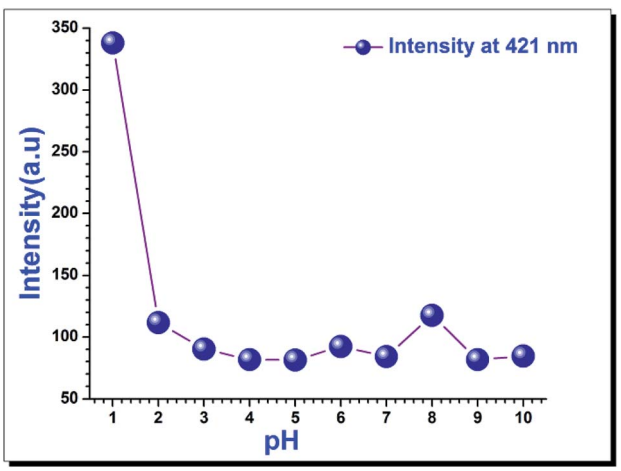

Fig. 6 Intensity of **1** (2 μM) at 421 nm being excited at 346 nm in buffer solutions of various pH ranges (1 to 10).

fluorescence intensity may be due to interaction of excited state of the fluorophore **1** with Cu^{2+} ion.

3.8. pH dependency of 1

For many biological applications, it is very important that the chemo-sensor shows no change in the physiological pH range.

Therefore, we investigated the effect of pH ranging from 1 to 10 (Fig. 6).[27] A sharp intensity change was observed between pH 1 to 2, but there was no appreciable change in the intensity beyond pH 2, except a minute increase at pH 8; the reason for this increase is not clear. To get the intensity changes of **1**, it was excited at 346 nm for all pH values.

3.9. Solvatochromism[38,39]

UV-vis absorption spectra and fluorescence emission spectra of **1** in a series of solvents of varying polarity are shown in Fig. 7. In aprotic solvents, the absorption maximum was progressively red shifted with increase in the polarity of the solvent, whereas for protic solvents it became blue shifted (Fig. 7a). On the other hand no considerable changes in the fluorescence emission maxima were observed in solvents of varying polarities. Although an increase in the fluorescence intensity was observed with increasing polarity of aprotic solvents, however there is a sharp decrease in emission intensity in case of the protic solvents (Fig. 7b). The fluorescence quenching in methanol and ethanol indicates the presence of an efficient non-radiative decay process from the emitting excited state of compound **1** in protic solvent. The increased probability of non-radiative decay may be attributed to the hydrogen bonding of N–H group with the protic solvents.[40]

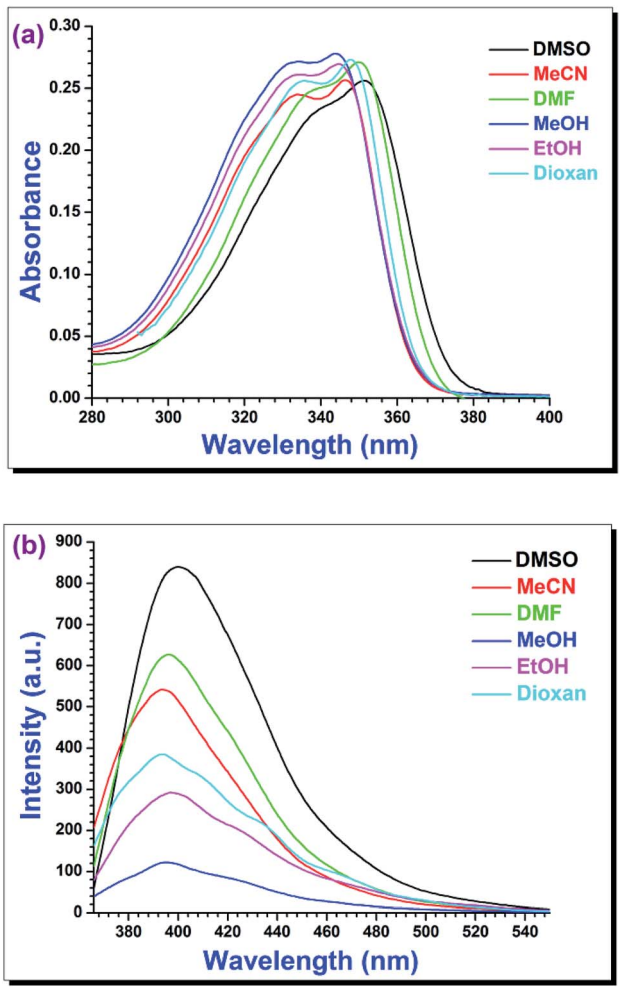

Fig. 7 (a) Absorption changes of **1** (7.2 μM) in various solvents at room temperature. (b) Intensity changes of **1** (0.5 μM) by exciting at 346 nm in various solvents at room temperature.

3.10. Antioxidant activity

This experiment is based on the extent of the scavenging capacity of antioxidant **1** towards 1,1-diphenyl-2-picrylhydrazyl (DPPH). The odd electron of N in DPPH is reduced by getting hydrogen atom from antioxidant **1** to the corresponding hydrazine.[41] While DPPH can accept hydrogen radical or an electron for getting stability, **1** is irreversibly oxidised. Due to having an odd electron, DPPH shows absorption maxima at 517 nm, and its solution appears deep violet, but the absorption vanishes when the electron pairs off. The methanolic solution of 50 μM DPPH is intensely coloured, and at this concentration, the Lambert–Beer's law is obeyed over the useful range of absorbance. Equation of free radical scavenging ratio:

$$\frac{\mathrm{Abs}_0 - \mathrm{Abs}_i}{\mathrm{Abs}_0} \times 100 = I\% \qquad (6)$$

where I% is percentage of scavenging, Abs_0 and Abs_i are the absorption values of DPPH solution without antioxidant **1**, and the absorbance of DPPH solution in the presence of antioxidant **1**, respectively. The IC_{50} value is the concentration of the antioxidant required for scavenging 50% DPPH and can be calculated from the inhibition curve using eqn (6). From the inhibition curve (Fig. 8) it can be better concluded that **1** has six times greater antioxidant capability than the well-known antioxidant L-ascorbic acid.

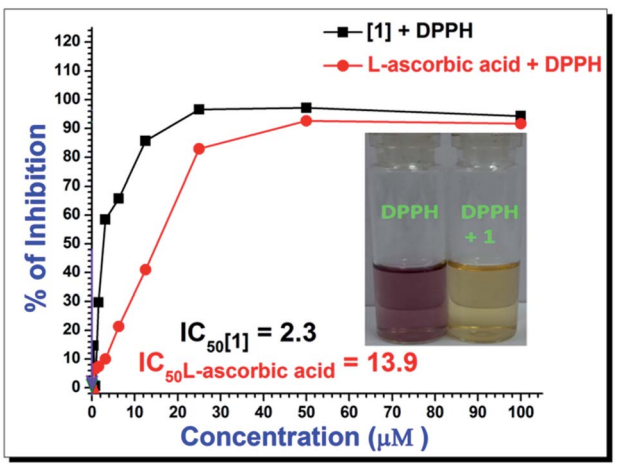

Fig. 8 Scavenging of DPPH radical by **1** (black) and L-ascorbic acid (red) in MeOH medium at room temperature. Inset: the colour change of methanolic solution of DPPH (50 μM) in the presence of **1** (1.5 μM) at room temperature.

3.11. Interaction of 1 with CT-DNA[28,29]

Upon the addition of aqueous CT-DNA to the solution of **1** in citrate-phosphate buffer medium of pH 7, there occurs a slight absorption changes with an isosbestic point at 292 nm (Fig. 9a). The presence of the isosbestic point gives a hint that there is equilibrium between the free **1** and the CT-DNA bound **1** in the ground state. A poor binding constant with value 4.6×10^2 M^{-1} at 357 nm (Fig. 9b) suggests groove binding of the **1** with CT-DNA. Furthermore, the fluorescence quenching spectra disclose the interaction of **1** with CT-DNA more precisely, and a low quenching efficiency (26%) also indicates the groove binding because intercalation of small molecules into the DNA base stack usually shows a huge change of the absorbance value as well as of fluorescence intensity.

We have then measured the circular dichroism (CD) spectra to ensure the mode of binding of **1** with CT-DNA. The secondary structure of DNA is recognized to be perturbed effectively by the intercalation with small molecules by giving the changes in the intrinsic CD spectrum of DNA, whereas groove binding of the small molecules has inconsiderable impact on the CD profile diagram of DNA. The CD spectra of CT-DNA prominently display that successive addition of **1** to the CT-DNA solution does not present any meaningful change in the CD spectrum of CT-DNA implying that the secondary structure of the CT-DNA remains unaffected on binding with **1**.

This investigation eliminates the chance of intercalation of **1** in the DNA helix, and hence establishes the groove binding mode.

4. Conclusion

In summary, we have developed a perimidine based new colorimetric sensor for the detection of aqueous Cu^{2+} ion, as the third most abundant transition metal ion in human bodies. The chemo-sensor **1** can also be used as a highly selective and sensitive, naked-eye and fluorescence turn-off sensor for aqueous Cu^{2+} ion; it enables analysis of aqueous Cu^{2+} ion with a detection limit of 6.19×10^{-8} M, which is below the WHO acceptable limit (31.5×10^{-3} M).[23] Moreover, the 1 : 1 interaction of **1** with Cu^{2+} was chemically irreversible in the presence of EDTA and CN^- which suggests strong binding between **1** and Cu^{2+}. Furthermore, **1** acts as a better antioxidant (six times) than L-ascorbic acid. We have also investigated the interaction of this chemo-sensor with calf-thymus DNA in the ground state as well as in the higher excited state and established the binding mode

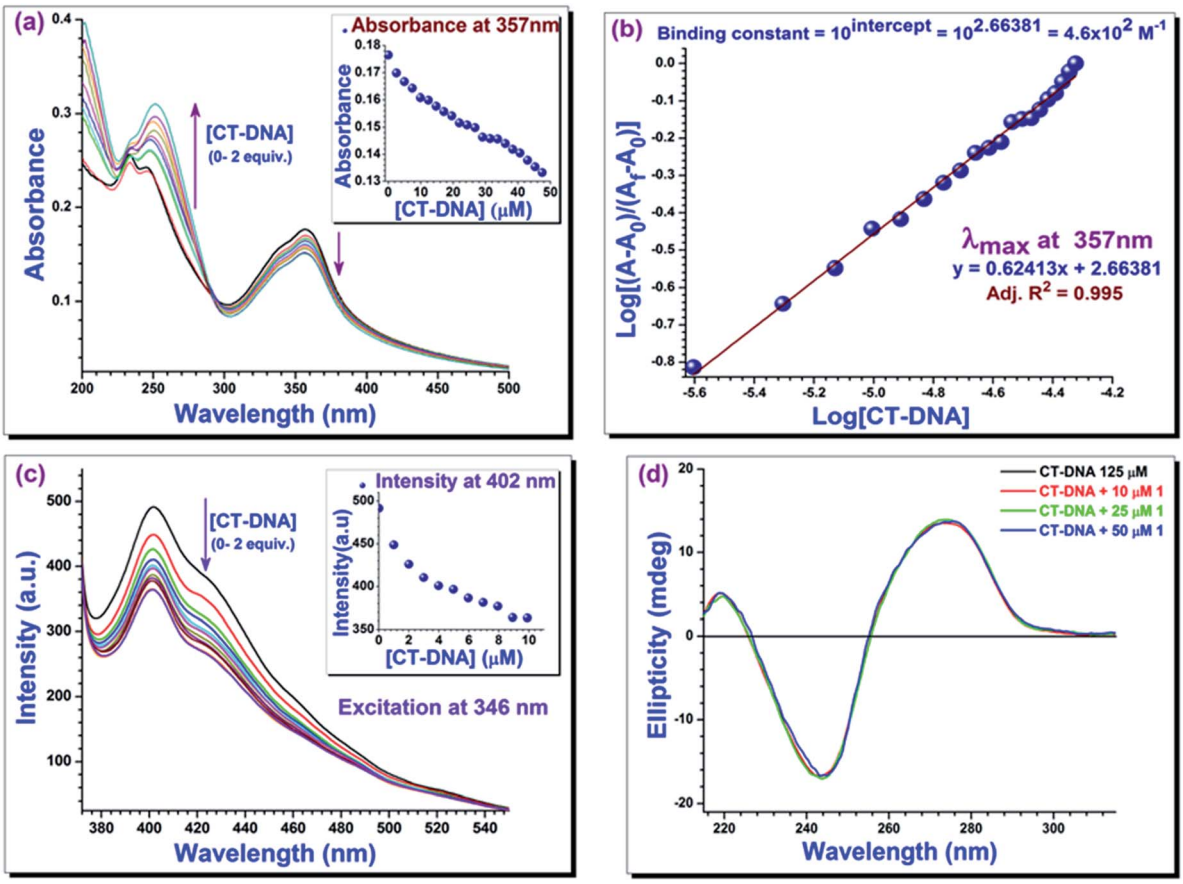

Fig. 9 (a) Spectral changes of **1** upon the addition of CT-DNA (upto 2 equiv.) at pH 7 buffer. Inset: absorbance changes of **1** at 357 nm as a function of CT-DNA concentration. (b) Benesi–Hildebrand plots for determination of binding constant of **1** for CT-DNA. (c) A fluorescent quenching of **1** in the presence of CT-DNA (upto 2 equiv.) at pH 7 buffer. Inset: intensity changes of **1** at 402 nm as a function of CT-DNA concentration. (d) Representative CD spectra of CT-DNA with various concentrations of **1** at room temperature.

of **1** in the DNA helix. Overall, the present work is a novel impute to the field of chemo-sensing.

Conflicts of interest

There are no conflicts of interest to declare.

Acknowledgements

Financial supports from SERB, DST, India (SR/FT/CS-116/2010) and CSIR, India (02/0186/14/EMR-II) are acknowledged, respectively by AC and RG. The authors are thankful to the Department of Chemistry, Maulana Azad College, Kolkata for supporting with some instrumental facilities and to FIST-DST and UGC-CAS, India for providing with the instrumental facilities in the Department of Chemistry, Jadavpur University.

References

1 D. Udhayakumari, S. Velmathi, Y. M. Sung and S. P. Wu, *Sens. Actuators, B*, 2014, **198**, 285–293.
2 P. L. Malvankar and V. M. Shinde, *Analyst*, 1991, **116**, 1081–1084.
3 H. Xu, X. Wang, C. Zhang, Y. Wu and Z. Liu, *Inorg. Chem. Commun.*, 2013, **34**, 8–11.
4 C. Vulpe, B. Levinson, S. Whitney, S. Packman and J. Gitschier, *Nat. Genet.*, 1993, **3**, 7–13.
5 P. C. Bull, G. R. Thomas, J. M. Rommens, J. R. Forbes and D. W. Cox, *Nat. Genet.*, 1993, **5**, 327–337.
6 R. Kramer, *Angew. Chem., Int. Ed.*, 1998, **37**, 772–773.
7 W. T. Tak and S. C. Yoon, KSN, 2001, **20**, 863–865.
8 J. W. Liu and Y. Lu, *J. Am. Chem. Soc.*, 2007, **129**, 9838–9839.
9 L. Kiaune and N. Singhasemanon, *Rev. Environ. Contam. Toxicol.*, 2011, **213**, 1–26.
10 A. Tong, Y. Akama and S. Tanaka, *Analyst*, 1990, **115**, 947–949.
11 T. Poursaberi, L. H. Babaei, M. Yousefi, S. Rouhani, M. Shamsipur, M. K. Razi, A. Moghimi, H. Aghabozorg and M. R. Ganjali, *Electroanalysis*, 2001, **13**, 1513–1517.
12 G. P. C. Rao, K. Seshaiah, Y. K. Rao and M. C. Wang, *J. Agric. Food Chem.*, 2006, **54**, 2868–2872.
13 M. Royzen, Z. H. Dai and J. W. Canary, *J. Am. Chem. Soc.*, 2005, **127**, 1612–1613.
14 Y. Zhao, X. B. Zhang and Z. X. Han, *Anal. Chem.*, 2009, **81**, 7022–7030.
15 S. J. Lee, J. E. Lee and J. Seo, *Adv. Funct. Mater.*, 2007, **17**, 3441–3446.
16 J. M. McCord, *Am. J. Med.*, 2000, **108**, 652–659.
17 A. Scalbert, C. Manach, C. Morand and C. Remsy, *Crit. Rev. Food Sci. Nutr.*, 2005, **45**, 287–306.
18 A. Shirwaikar, A. Shirwaikar, R. Kuppusamy and S. R. Isaac, *Biol. Pharm. Bull.*, 2006, **29**, 1906–1910.
19 B. Halliwell and J. M. C. Gutteridge, *Free radicals in biology and medicine*, Oxford University Press, Oxford, 2000.
20 F. Anwar, M. Ali, A. I. Hussain and M. Shahid, *Flavour Fragrance J.*, 2009, **24**, 170–176.
21 J. Deng, W. Cheng and G. Yang, *Food Chem.*, 2011, **125**, 1430–1435.
22 I. G. Jung, S. U. Son, K. H. Park, K. C. Chung, J. W. Lee and Y. K. Chung, *Organometallics*, 2003, **22**, 4715–4720.
23 H. Y. Jo, G. J. Park, Y. J. Na, Y. W. Choi, G. R. You and C. Kim, *Dyes Pigm.*, 2014, **109**, 127–134.
24 R. L. Liu, H. Y. Lu, M. Li, S. Z. Hu and C. F. Chen, *RSC Adv.*, 2012, **2**, 4415–4420.
25 H. Xu, X. Wang, C. Zhang, Y. Wu and Z. Liu, *Inorg. Chem. Commun.*, 2013, **34**, 8–11.
26 G. K. Li, Z. X. Xu, C. F. Chen and Z. T. Huang, *Chem. Commun.*, 2008, 1774–1776.
27 J. Reijenga, A. V. Hoof, A. V. Loon and B. Teunissen, *Anal. Chem. Insights*, 2013, **8**, 53–71.
28 P. Kundu, S. Ghosh and N. Chattopadhyay, *Phys. Chem. Chem. Phys.*, 2015, **17**, 17699–17709.
29 D. Sarkar, P. Das, S. Basak and N. Chattopadhyay, *J. Phys. Chem. B*, 2008, **112**, 9243–9249.
30 R. M. Duke, E. B. Veale, F. M. Pfeffer, P. E. Kruger and T. Gunnlaugsson, *Chem. Soc. Rev.*, 2010, **39**, 3936–3953.
31 A. Misra, M. Shahid, P. Dwivedi, P. Srivastava, R. Ali and S. S. Razi, *ARKIVOC*, 2013, **ii**, 133–145.
32 M. Dong, T. H. Ma, A. J. Zhang, Y. M. Dong, Y. W. Wang and Y. Peng, *Dyes Pigm.*, 2010, **87**, 164–172.
33 J. Li, H. Lin, Z. Cai and H. Lin, *J. Lumin.*, 2009, **129**, 501–505.
34 F. U. Rahman, A. Ali, S. K. Khalil, R. Guo, P. Zhang, H. Wang, Z. T. Li and D. W. Zhang, *Talanta*, 2017, **164**, 307–313.
35 A. B. Pradhan, S. K. Mandal, S. Banerjee, A. Mukherjee, S. Das, A. R. K. Bukhsh and A. Saha, *Polyhedron*, 2015, **94**, 75–82.
36 W. H. Melhuish, *J. Phys. Chem.*, 1961, **65**, 229–235.
37 D. F. Eaton, *Pure Appl. Chem.*, 1988, **60**, 1107–1114.
38 J. Jayabharathi, V. Thanikachalam, M. V. Perumal and K. Jayamoorthy, *J. Fluoresc.*, 2012, **22**, 213–221.
39 S. Cha, M. G. Choi, H. R. Jeon and S. K. Chang, *Sens. Actuators, B*, 2011, **157**, 14–18.
40 J. D. Cheon, T. Mutai and K. Araki, *Org. Biomol. Chem.*, 2007, **5**, 2762–2766.
41 S. B. Kedare and R. P. Singh, *J. Food Sci. Technol.*, 2011, **48**, 412–422.

